

3-21-2012

A Ceramic-Anode Supported Low Temperature Solid Oxide Fuel Cell

Hanping Ding

Junjie Ge

Xingjian Xue

University of South Carolina - Columbia, xue@cec.sc.edu

Follow this and additional works at: https://scholarcommons.sc.edu/emec_facpub

 Part of the [Electro-Mechanical Systems Commons](#), [Energy Systems Commons](#), and the [Power and Energy Commons](#)

Publication Info

Published in *Electrochemical and Solid-State Letters*, Volume 15, Issue 6, 2012, pages B86-B89.

©Electrochemical and Solid-State Letters 2012, The Electrochemical Society.

© The Electrochemical Society, Inc. 2012. All rights reserved. Except as provided under U.S. copyright law, this work may not be reproduced, resold, distributed, or modified without the express permission of The Electrochemical Society (ECS). The archival version of this work was published in *Electrochemical and Solid-State Letters*.

Publisher's Version: <http://dx.doi.org/10.1149/2.019206esl>

Ding, H., Ge, J., & Xue, X. (21 March 2012). A Ceramic-Anode Supported Low Temperature Solid Oxide Fuel Cell. *Electrochemical and Solid-State Letters*, 15 (6), B86 – B89. <http://dx.doi.org/10.1149/2.019206esl>



A Ceramic-Anode Supported Low Temperature Solid Oxide Fuel Cell

Hanping Ding, Junjie Ge, and Xingjian Xue^{*,z}

Department of Mechanical Engineering, University of South Carolina, Columbia, South Carolina 29208, USA

We report the fabrication and evaluation of a ceramic-anode supported button cell LSCM-SDC/SDC/PBSC (thickness 400 μm /20 μm /20 μm). The anode/electrolyte assembly LSCM-SDC/SDC was co-fired at low temperature of 1250°C, where a slight amount of CuO was mixed with LSCM. The CuO (20.3 wt%) were impregnated into the porous substrate to enhance current collecting effect. The cell exhibited power density of 596 mWcm^{-2} and 381 mWcm^{-2} at 700°C with wet hydrogen and methane as the fuel respectively, where the silver paste was used as current collectors, the highest performance up to date for the cells with metal oxide anodes at this temperature.

© 2012 The Electrochemical Society. [DOI: 10.1149/2.019206es] All rights reserved.

Manuscript submitted January 9, 2012; revised manuscript received March 7, 2012. Published March 21, 2012.

The carbon deposition and sulfur poisoning are two major obstacles for hydrocarbon fueled SOFCs with nickel cermet anode.^{1,2} In addition, the nickel based anodes also suffer from the volume instability induced by redox cycling³ as well as nickel particle agglomerations due to high temperature and long-term operations.⁴ To overcome these issues, nickel-free metal oxide anode materials have been investigated, such as $\text{La}_{0.75}\text{Sr}_{0.25}\text{Cr}_{0.5}\text{Mn}_{0.5}\text{O}_{3-8}$ (LSCM),⁵ $\text{Sr}_2\text{Mg}_{1-x}\text{Mn}_x\text{MoO}_{6-8}$ ($x = 0$ to 1),⁶ and doped (La, Sr)(Ti)O₃.^{7,8} Experimental results have demonstrated that such anode materials are effective in inhibiting carbon deposition or sulfur poisoning.⁹⁻¹¹

So far the cell designs are exclusively electrolyte-supported when metal oxide anodes are employed. This design requires relatively thick electrolyte of 300~500 μm to support the entire cell, leading to significant ohmic resistance. Accordingly, high temperatures (800–900°C) are needed to reduce the ohmic loss for high power outputs. The high operating temperatures in turn could lead to a variety of degradations. Anode-supported designs may effectively reduce the ohmic loss with thin electrolyte membrane while lowering the operating temperatures, which have been well demonstrated with nickel cermet anode. However, the anode-supported designs with metal oxides as anode materials are difficult to fabricate. In general, high sintering temperature is needed to co-fire the anode substrate/electrolyte assembly to densify the thin electrolyte, which in turn may induce the densification of the porous anode substrate, resulting in anode porosity loss. Another issue is that the existing oxide anode materials cannot provide adequate conductivity for current collection in thick anode substrate.

Here we report the development of anode-supported intermediate temperature (550–700°C) SOFC with metal oxide LSCM as the supporting substrate, $\text{Sm}_{0.2}\text{Ce}_{0.8}\text{O}_2$ (SDC) as the electrolyte, and $\text{PrBa}_{0.5}\text{Sr}_{0.5}\text{Co}_2\text{O}_{5+\delta}$ (PBSC) as the cathode. With a slight amount of CuO mixed with LSCM, the anode substrate/electrolyte assembly was co-fired at low temperature of 1250°C. The dense thin SDC electrolyte (20 μm) was obtained while the sufficient porosity of anode substrate (400 μm) was maintained. The CuO nano-particles (20.3 wt%) were impregnated into the porous substrate to enhance current collecting effect of thick anode. The cell exhibited the volumetric power density of 596 mW cm^{-2} and 381 mW cm^{-2} at 700°C with wet hydrogen and methane as the fuel respectively, where the silver paste was used as current collector, the highest performance up to date for the cells with metal oxide anodes at this temperature.

Experimental

The $\text{La}_{0.75}\text{Sr}_{0.25}\text{Cr}_{0.5}\text{Mn}_{0.5}\text{O}_{3-8}$ powders were synthesized by modified Pechini method. Briefly citrate and ethylenediamine tetraacetic acid (EDTA) were employed as parallel complexing agents. La_2O_3 was calcined at 1000°C for 5 h to remove the humid water, and

then dissolved in nitric acid. The stoichiometric amounts of $\text{Sr}(\text{NO}_3)_2$ (99.99%), $\text{Cr}(\text{NO}_3)_3 \cdot 9\text{H}_2\text{O}$ (99.99%) and $\text{Mn}(\text{CH}_3\text{COO})_2 \cdot 4\text{H}_2\text{O}$ (99.99%) were dissolved in EDTA-NH₃ aqueous solution. After agitation for a certain period of time, a proper amount of citric acid was introduced, the molar ratio of EDTA : citric acid : total of metal cations was controlled around 1:1.5:1. After converted into viscous gel under heating and stirring conditions, the solution was ignited to flame and result in ash. The resulting ash-like material was afterwards calcined in air at 1200°C for 5 h to obtain LSCM powders. The $\text{Sm}_{0.2}\text{Ce}_{0.8}\text{O}_2$ and $\text{PrBa}_{0.5}\text{Sr}_{0.5}\text{Co}_2\text{O}_{5+\delta}$ powders were synthesized using the same method.

The specimens of SDC-LSCM rectangular bar (60 mm \times 5 mm \times 1.8 mm) were fabricated by dry-pressing method with a stainless steel die at 360 MPa and sintered at 1250°C for 5 h in air. The rectangular bar was then infiltrated by copper nitrate solution and fired at 600°C for 30 min with heating/cooling rate of 10°C min⁻¹ to decompose nitrate. The electrical conductivities of SDC-LSCM with/without Cu infiltration were studied from 400°C to 800°C in the atmosphere of 5% H₂/95% Ar by a standard DC four-probe technique with a multimeter (Agilent, 34401A). The LSCM-SDC/SDC bi-layer cells ($\Phi = 15$ mm) were prepared by dry-pressing/co-firing method. The mixture of CuO + LSCM + SDC + starch, with the ratio of CuO:LSCM:SDC:starch = 1:12:8:6 in weight, was pre-pressed at 200 MPa to form an anode substrate. Then loose SDC powder was uniformly distributed onto the anode substrate, co-pressed at 250 MPa and sintered subsequently at 1250°C for 6 h to densify the SDC membrane. The cell Cu-SDC/SDC was fabricated by the same method and sintered at 1100°C for 2 h. The thickness of each layer is controlled to be similar to those of Cu-LSCM-SDC/SDC cell. The Cu was then infiltrated into the porous anode substrate. Briefly, the nitrate solution was prepared by dissolving $\text{Cu}(\text{NO}_3)_2 \cdot 2.5\text{H}_2\text{O}$ in distilled water. The solution was dropped onto the substrate surface and infiltrated into the porous anode. After drying, the samples were fired at 600°C for 30 min with heating and cooling rate of 10°C min⁻¹ to decompose nitrate. The final CuO loading was about 20.3 wt% of total anode substrate after four infiltration-heating cycles. The cathode slurry was prepared by mixing PBSC powders with a 6 wt% ethylcellulose-terpineol binder. The slurry was then painted on SDC electrolyte, and sintered at 1000°C for 3 h in air to form single cells of Cu-LSCM-SDC/SDC/PBSC. The silver paste was then painted on the anode and cathode respectively and dried as current collector.

The cells with Cu-SDC-LSCM and Cu-SDC anodes were tested from 550 to 700°C with humidified hydrogen and methane (~3% H₂O) as fuels respectively and the static air as the oxidant. The flow rate of the fuel was controlled at 40 mL/min by a mass flowmeter (APEX). The voltage-current curves were recorded by Scribner 890ZV at a scanning rate of 50 mV s⁻¹. The electrochemical impedance spectra (EIS) were obtained using a Solartron 1260 frequency response analyzer in combination with a Solartron 1287 potentiostat over the frequency range from 0.1 Hz to 10⁵ Hz under

*Electrochemical Society Active Member.

^zE-mail: Xue@cec.sc.edu

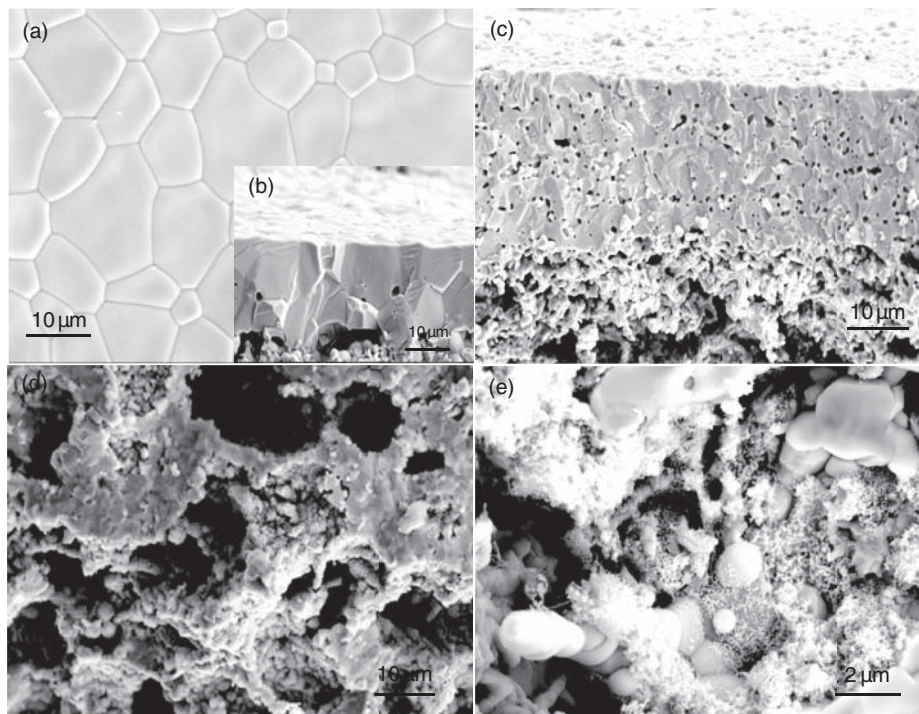


Figure 1. SEM images of cell after sintering: (a) the surface of electrolyte; (b) the cross-section of cell with a 20 μm thick SDC membrane; (c) the cross-section of cell without CuO sintering additive; (d) the porous anode morphology after ion-impregnation; (e) the Cu nanoparticles coating on LSCM-SDC surfaces.

open-circuit conditions. A scanning electron microscope (SEM, Zeiss) was used to observe the microstructure of the cells. The porosity of anode was measured using mercury porosimeter (AutoPore IV).

Results and Discussion

Figure 1a and 1b show the SEM images of the fabricated LSCM-anode supported single cell. Apparently SDC electrolyte was dense while keeping sufficient porosity of substrate (35.05%). And the average grain size of SDC electrolyte was about 10 μm , far bigger than those of NiO-SDC/SDC cells co-sintered at 1400°C.¹²⁻¹⁴ It is anticipated that the large grain size may reduce the resistance induced by grain boundaries and improve the conductivity of the electrolyte. The CuO plays an important role in lower temperature (1250°C) co-firing while achieving high quality sintering results.¹⁵ As a comparison, the substrate/electrolyte assembly without addition of CuO was also co-sintered at the same temperature of 1250°C. The corresponding SEM is shown in Figure 1c. Obviously, the electrolyte membrane was not dense and a large portion of porosity exists. The growth of SDC grains was also severely inhibited.

The thick anode substrate of oxide LSCM may lead to inadequate conductivity particularly at lower operating temperature conditions, therefore metal Cu was introduced into porous anode substrate by ion-impregnation method to improve the current collecting effect. Figure 1d shows the porous anode substrate impregnated with Cu, where the nano-sized fine copper particles form a highly interconnected network structure, providing continuous electron-conducting paths (Figure 1e).

Figure 2a shows the polarization and power density curves of the cell with infiltrated anode at the temperatures of 550–700°C. The humidified hydrogen ($\sim 3\%$ H₂O) and ambient air were used as the fuel and the oxidant respectively. The open circuit voltage (OCV) at 550, 600, 650 and 700°C was 0.9, 0.88, 0.86 and 0.85 V respectively, indicating that the electrolyte is sufficient dense. Due to the partial reduction of Ce⁴⁺ to Ce³⁺ in SDC when exposed to a low oxygen partial pressure (1×10^{-19} atm) and temperature ($>600^\circ\text{C}$), a slight electronic current leakage might exist.¹⁶ However, the OCVs observed from this experiment are slightly higher than those reported in literature¹⁷ and are in good agreement with microstructure images

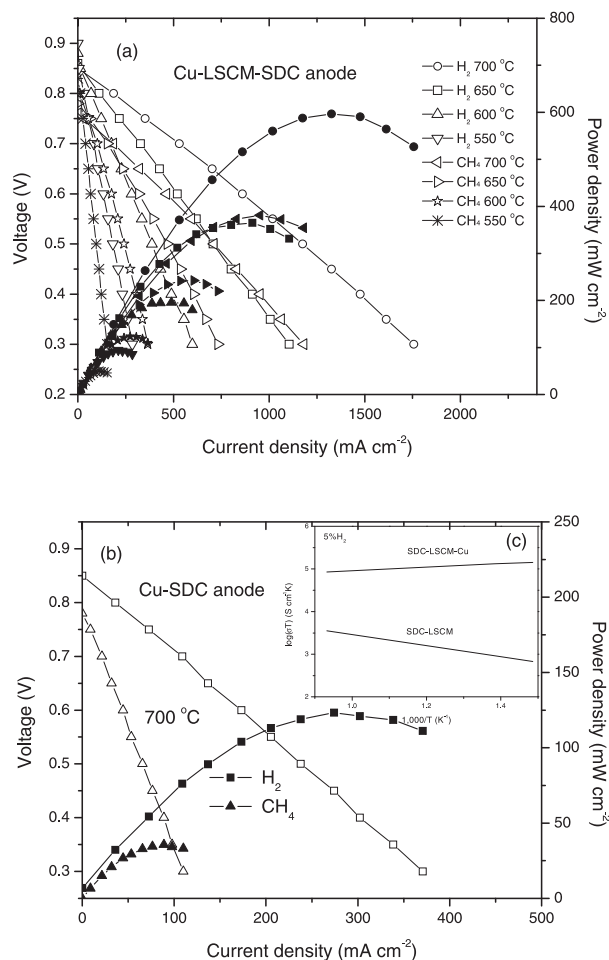


Figure 2. Cell voltage and power density as a function of current density (a) Cu-LSCM-SDC/SDC/PBSC and (b) Cu-SDC/SDC/PBSC with H₂ and CH₄ as fuel, respectively; (c) The conductivities of LSCM-SDC and Cu infiltrated LSCM-SDC anode in 5% H₂/95% Ar.

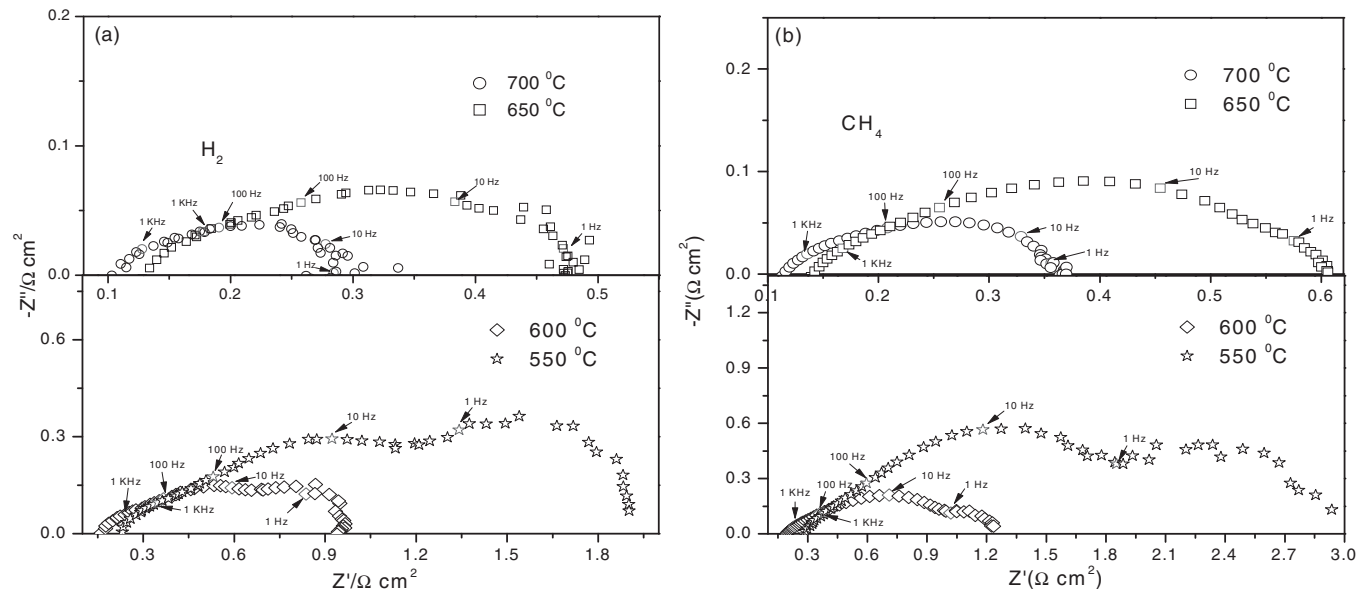


Figure 3. Impedance spectra measured under open-circuit conditions at different temperatures with (a) H₂ and (b) CH₄ as fuels, respectively.

in Figure 1. The maximum power density was 596, 365, 196 and 94 mW cm⁻² at 700, 650, 600 and 550 °C, respectively. With wet CH₄ as the fuel, the maximum power density reached 381 mW cm⁻² at 700 °C. In the 300 μm-thick YSZ electrolyte-supported cell with pure LSCM as the anode,⁵ the cell exhibited the peak power densities of 470 mW cm⁻² in wet H₂ and 200 mW cm⁻² in CH₄ at 900 °C, respectively. In a recent study,⁶ a 300 μm-thick La_{0.8}Sr_{0.2}Ga_{0.83}Mg_{0.17}O₃ (LSGM) electrolyte-supported cell with double perovskite Sr₂MgMoO₆ anode showed the peak power density of 438 mW cm⁻² at 800 °C in CH₄. The cell performance reported in this study is very encouraging because the cell obtained high performance in relatively low temperatures. Figure 2b shows the performance of cell Cu-SDC/SDC without LSCM. At 700 °C, the maximum power density was 123 mW cm⁻² in H₂ and 36 mW cm⁻² in CH₄ which were much lower than those of the cell with LSCM. The results indicate that catalytic property of Cu is poor and LSCM plays an important catalytic role in the anode. The conductivities of LSCM-SDC with and without Cu infiltration are shown in Figure 2c. The LSCM-SDC bar exhibited the conductivity of only 1 S/cm at 400 °C and 3.28 S/cm at 800 °C. After Cu infiltration, the conductivity was significantly improved to 210 S/cm at 400 °C and 79 S/cm at 800 °C respectively.

To evaluate the performance of the thin electrolyte and Cu-impregnated anode in the whole fuel cell, the impedance spectra of the as-prepared cell were measured under open-circuit conditions with wet hydrogen and CH₄ as fuels at different temperatures. The results are shown in Figure 3. In these spectra, the low frequency intercept represents the total resistance (R_t) of the cell; the high frequency intercept is the total ohmic resistance (R_o) contributed mainly by the electrolyte; the difference between R_t and R_o corresponds to the electrode polarization resistance (R_p), including the contributions from both the anode and cathode.¹⁸ As shown in Figure 3a, the electrolyte resistance was only 0.23, 0.16, 0.12 and 0.1 Ω cm² at 550, 600, 650 and 700 °C, respectively. By contrast, the LSGM electrolyte-supported cell (~300 μm in thickness) showed the ohmic resistance of 0.78 Ω cm² at 700 °C.¹⁹ The cell ohmic resistance didn't show apparent changes when the fuel was switched to the methane (Figure 3b). Obviously the application of thin film electrolyte in anode-supported cells resulted in a significant reduction of ohmic resistance. With H₂ as the fuel, the total polarization resistance R_p was 1.67, 0.79, 0.37 and 0.2 Ω cm² at 550, 600, 650 and 700 °C, respectively. With CH₄ as the fuel, the R_p value increased to 0.28 Ω cm² at 700 °C. As a comparison, the polarization resistance of anode with pure LSCM was 0.26 Ω cm²

in wet H₂ and 0.87 Ω cm² in wet CH₄ at 900 °C, respectively.⁵ It is worth mentioning that the anode polarization resistance was measured using a three-electrode configuration in the latter case. Considering that the polarization resistance contributed from the cathode was also included in our measurement results, the actual polarization resistance of the anode will be even lower than those values mentioned above. These results indicate that the LSCM anode impregnated with Cu may effectively improve the anode polarization performance even though the thick LSCM substrate was used.

Conclusions

In this study, we first examined the feasibility of ceramic LSCM anode supported SOFC fabrication. With a slight amount of CuO addition to the substrate, the dense electrolyte SDC and anode substrate LSCM with sufficient porosity were obtained by co-sintering LSCM/SDC assembly at low temperature 1250 °C. Second, by infiltrating CuO nano-particle into porous substrate, current collection was improved for the ceramic anode LSCM. As a result, we can fabricate anode-LSCM-supported SOFCs at low sintering temperature with high volumetric power density of 596 mW cm⁻² and 381 mW cm⁻² at 700 °C with wet hydrogen and methane as the fuel respectively, the highest performance up to date for the cells with metal oxide anodes at this temperature.

References

1. S. McIntosh and R. J. Gorte, *Chem. Rev.*, **104**, 4851 (2004).
2. J. T. S. Irvine, *Perovskite oxides anodes for solid oxide fuel cells*, Springer, New York, p. 167 (2009).
3. Q. X. Fu, F. Tietz, and D. Stöver, *J. Electrochem. Soc.*, **153**, D74 (2006).
4. R. Vassen, D. Simwonis, and D. Stöver, *J. Mater. Sci.*, **36**, 147 (2001).
5. S. W. Tao and J. T. S. Irvine, *Nat. Mater.*, **2**, 320 (2003).
6. Y. H. Huang, R. I. Dass, Z. L. Xing, and J. B. Goodenough, *Science*, **312**, 254 (2006).
7. J. C. Ruiz-Morales, J. Canales-Vázquez, C. Savaniu, D. Marrero-López, W. Z. Zhou, and J. T. S. Irvine, *Nature*, **439**, 568 (2006).
8. O. A. Marina, N. L. Canfield, and J. W. Stevenson, *Solid State Ionics*, **149**, 21 (2002).
9. J. B. Goodenough and Y. H. Huang, *J. Power Sources*, **173**, 1 (2007).
10. R. J. Gorte, J. M. Vohs, and S. McIntosh, *Solid State Ionics*, **175**, 1 (2004).
11. Y. H. Huang, G. Liang, M. Croft, M. Lehtimäki, M. Karppinen, and J. B. Goodenough, *Chem. Mater.*, **21**, 2319 (2009).
12. M. Chen, B. H. Kim, Q. Xu, B. G. Ahn, and D. P. Huang, *J. Membrane Sci.*, **360**, 461 (2010).

13. N. Ai, Z. Lü, K. F. Chen, X. Q. Huang, Y. W. Liu, R. F. Wang, and W. H. Su, *J. Membrane Sci.*, **286**, 255 (2006).
14. C. R. Xia and M. L. Liu, *Solid State Ionics*, **144**, 249 (2001).
15. J. D. Nicholas and L. C. D. Jonghe, *Solid State Ionics*, **178**, 1187 (2007).
16. M. H. D. Othman, N. Droushiotis, Z. T. Wu, G. Kelsall, and K. Li, *Adv. Mater.*, **23**, 2480 (2011).
17. N. Ai, Z. Lü, K. F. Chen, X. Q. Huang, B. Wei, Y. H. Zhang, S. Y. Li, X. S. Xin, X. Q. Sha, and W. H. Su, *J. Power Sources*, **159**, 637 (2006).
18. H. P. Ding, B. Lin, X. Q. Liu, and G. Y. Meng, *Electrochem. Commun.*, **10**, 1388 (2008).
19. G. L. Xiao, Q. Liu, X. H. Dong, K. Huang, and F. L. Chen, *J. Power Sources*, **195**, 8071 (2010).